An Optimization-Based Reduced Sensor Virtual Flux Observer for PM Synchronous Machines

Michael Eull and Matthias Preindl, *Senior Member, IEEE*

***Abstract*—Cost remains a major obstacle to the widespread adoption of electrified vehicles. Significant research effort has been expended in trying to replace hardware with software in systems in an effort to bring it down. To accomplish this, phase current estimation has emerged as a viable means of removing sensors from electric drives. The plurality of work in the field employs linear current observers, which suffer from a need for machine anisotropy and periodic position-dependent non-observability, both of which limit applicability. This paper proposes an optimization-based methodology that eliminates all estimation constraints. It is shown that the problem is always at least quasiconvex, permitting the estimation of the *dq* fluxes under a set of operating constraints. By way of an additional term in the cost function, the problem is made strictly convex for all operating conditions, enabling efficient estimation of the unique *dq* fluxes. Experiments validate the concept and show that the optimization-based observer performs similarly to the linear observer in the steady state with ringing after transients reduced.**

***Index Terms*—Observers, estimation, permanent magnet machines**

I. Introduction

A major impediment to the development and adoption of electrified vehicles has been and remains the cost. One of the most promising ways to reduce cost has been to supplant hardware with software [1]. Two of the more popular examples of such an act are the removal of the position [2]–[5] or current [6]–[15] sensor(s) in the drive of an electrified vehicle.

The traditional current estimation problem has primarily landed within two overarching categories: reduced sensor (two or one) and sensorless. In the reduced sensor camp, these are further sub-divided into estimation via a DC-link current sensor [6]–[9] and estimation via phase current sensors [10]–[13], both with some underlying algorithm present. In the sensorless camp, these have tended to rely on an algorithm [14] or a precise model [15]. Current sensorless estimation suffers from parameter sensitivity issues, making reduced sensor techniques attractive for their ability to compensate for inevitable modelling errors and parameter variation while still seeing system cost reductions. Phase current estimation as a whole is a promising approach as it avoids the problems associated with estimation via the DC-link current, such as added inductance and the need for an expensive, high bandwidth sensor.

Manuscript received September 12, 2019; revised December 5, 2019 and February 3, 2020; accepted February 25, 2020.

The authors are with the Department of Electrical Engineering, Columbia University in the City of New York, New York, NY 10027, USA (e-mail: michael.eull@columbia.edu; matthias.preindl@gmail.com).

Typical three-phase electric drives employ three current sensors, where one is redundant to meet standards requiring redundancy, such as ISO 26262: Road vehicles — Functional safety. Recent work has seen a push towards removing the redundant sensor and adding a current observer as a fail safe to guard against a failure that results in insufficient information to control the system [10]–[13]. Given the low probability of a current sensor failure (one popular current sensor series has a mean time between failure of over two million hours [16]), the removal of one sensor and implementation of an observer is a clear choice for realizing a cost savings whilst simultaneously satisfying mandated redundancy requirements.

A reduction in cost through sensor removal comes at the expense of a degradation in performance relative to a two sensor system, where a one sensor linear observer PMSM drive exhibits: overshoot in the step response and associated transient settling time, both of which become more pronounced with parameter error due to one eigenvalue of the closed-loop system being determined by the machine's $\frac{L}{R}$ time constant; and a small increase in the steady state current ripple. In terms of robustness, both the two and one sensor linear observers can be made stable with appropriate feedback gain selection; however, the one sensor observer imposes requirements for estimability tied to the type of PMSM and the rotor's position, whereas the currents are always estimable with two sensors [13]. For low cost systems where torque quality is not critical or ones where performance can be derated in case of a sensor failure, these degradations may be an acceptable tradeoff.

The existing phase current observers in literature are designed with a linear Luenberger observer [10]–[13], which is iterative by nature and requires several sampling intervals to converge. Optimization-based approaches offer the promise of instantaneous estimation, compatibility with nonlinear models and enhanced performance over more traditional techniques, such as a linear Luenberger observer. Indeed, optimization has been shown to be an effective and efficient tool for many control and estimation problems [3]–[5], [17]–[19].

However, the employment of optimization techniques for estimating the missing quantities resulting from the removal of sensors has largely been restricted to the position sensorless problem [3]–[5]. While a position sensorless scheme could realize a greater cost savings than a current observer, it affords no redundancy and introduces risk, whereas a current observer can realize a guaranteed cost savings with minimal risk, owing to the redundancy it provides as a fail safe. Therefore, this work seeks to extend the optimization methodology beyond position estimation to flux (current) estimation, with a focus on estimation with only one phase current sensor.

This article has been accepted for publication in a future issue of this journal, but has not been fully edited. Content may change prior to final publication. Citation information: DOI 10.1109/TIE.2020.2982105, IEEE Transactions on Industrial Electronics

Relative to previous reduced current sensor research, the presented optimization-based virtual flux observer sees one major benefit: there are no restrictions on estimation. In [13], the conditions for observability were derived and found to require the PMSM to be anisotropic, meaning only interior PMSMs could benefit from the method; moreover, non-observability was found to be position-dependent and, while more of a theoretical than a practical limitation, estimation accuracy could be limited close to these points. The proposed optimization-based virtual flux observer, on the other hand, natively eliminates the anisotropy requirement, making the method applicable to both interior and surface mount PMSMs. When the cost function is augmented with an additional term, the position dependency is also removed and the fluxes (currents) are always estimable. In terms of quantifiable metrics, the optimization-based methodology exhibits similar rise time and steady state RMS ripple current when compared to the other reduced sensor phase current observers in literature [10]–[13]. An added benefit sees ringing after transients reduced.

II. Problem Formulation

The formulation of the virtual flux observer follows closely that of the position observer presented in [5].

The discrete-time state-space equations can be written as

$$x^+ = f\left(x, u, p\right) \tag{1a}$$

$$y = g\left(x, p\right), \tag{1b}$$

where x, u and p are vectors of the states, inputs and parameters of the system, respectively; x^+ is the state vector at the next time step; and y is the output of the system at the current time step. These two functions describe the input-output relationship, be it linear or nonlinear, of the system. The size of each vector is: $x^+ \in \mathbb{R}^{m\times 1}$, $x \in \mathbb{R}^{m\times 1}$, $p \in \mathbb{R}^{l\times 1}$, $u \in \mathbb{R}^{n\times 1}$, $y^+ \in \mathbb{R}^{r\times 1}$ and $y \in \mathbb{R}^{r\times 1}$, where m, l, n and r designate the number of states, parameters, inputs and outputs of the system, respectively.

An observer estimates the states of a system by way of its inputs and the resultant outputs. These states are intrinsically linked to the parameters of the system p, some of which may also be unknown. Thus, estimating the states can also be a problem of estimating the system's parameters. It becomes beneficial, then, to define a combined vector linking them together. Therefore, let $z = \begin{bmatrix}\left(x^+\right)^T & x^T & p^T\end{bmatrix}^T \in \mathbb{R}^{(2m+l)\times 1}$.

The vectors x^+, x and p can then be written as the product of a matrix and the state-parameter vector z, which extracts the relevant components. In this way, the vectors of interest are: $x^+ = \begin{bmatrix}\mathbf{I}_{m\times m}, & \mathbf{0}_{m\times(m+l)}\end{bmatrix} z$, $x = \begin{bmatrix}\mathbf{0}_{m\times m}, & \mathbf{I}_{m\times m}, & \mathbf{0}_{m\times l}\end{bmatrix} z$ and $p = \begin{bmatrix}\mathbf{0}_{l\times 2m}, & \mathbf{I}_{l\times l}\end{bmatrix} z$. $\mathbf{I}$ and $\mathbf{0}$ are identity and zero matrices, respectively.

Recalling the system described in (1), a function comprised of the outputs y, the inputs u and the state-parameter vector z can be built with the form

$$h\left(y, y^+, u, z\right) = \begin{bmatrix} f\left(x, u, p\right) - x^+ \\ g\left(x, p\right) - y \\ g\left(x^+, p\right) - y^+ \end{bmatrix} = 0. \tag{2}$$

where $h \in \mathbb{R}^{(m+2r)\times 1}$.

Note that an additional equation has been added when comparing (1) and (2). This extra equation allows for direct comparison between the estimated next-step state and the actual value measured, providing more information to the estimator. Note also the constraint placed on the function: that every term should be equal to zero. This is equivalent to stating that the estimates must match the measurements.

The last component required in the formulation is a cost function, whose minima imply the minima of h. A quadratic form is beneficial as it makes the function quadratic, which permits easier study of its convexity and a simpler means of solving. Because some z is being estimated to satisfy h, it becomes notationally convenient to use the widely-accepted circumflex above a variable to denote an estimate, such that z becomes $\hat{z}$. The cost function is then written as

$$c = h\left(y, y^+, u, \hat{z}\right)^T \mathbf{N} h\left(y, y^+, u, \hat{z}\right), \tag{3}$$

where $\mathbf{N}$ is a square positive definite weighting matrix and is used to give different weightings to terms in the cost function. Per (2), $\mathbf{N} \in \mathbb{R}^{(m+2r)\times(m+2r)}$.

The optimization problem can then be written as

$$z^* = \underset{\hat{z}}{\text{minimize}} \quad c\left(\hat{z}\right), \tag{4}$$

which is equivalent to stating that some optimal variable(s) z^* are sought that minimize the cost function c.

A. Key Mathematical Tools

The Jacobian is a matrix of the first partial derivatives of an equation. Its key use in this work is to determine whether the system at hand is identifiable; i.e. whether the states can be uniquely estimated. The Jacobian is

$$\mathbf{J}_h = \begin{bmatrix} \frac{\partial h_1}{\partial z_1} & \frac{\partial h_1}{\partial z_2} & \cdots & \frac{\partial h_1}{\partial z_n} \\ \frac{\partial h_2}{\partial z_1} & \frac{\partial h_2}{\partial z_2} & \cdots & \frac{\partial h_2}{\partial z_n} \\ \vdots & \vdots & \ddots & \vdots \\ \frac{\partial h_n}{\partial z_1} & \frac{\partial h_n}{\partial z_2} & \cdots & \frac{\partial h_n}{\partial z_n} \end{bmatrix}. \tag{5}$$

The Hessian is a matrix of the second derivatives of a function. It finds use in not only the act of optimization (e.g. Newton's method), but also in determining the convexity of the problem. The Hessian is computed as [5]

$$\mathbf{H}_c = \begin{bmatrix} \frac{\partial^2 c}{\partial z_1^2} & \frac{\partial^2 c}{\partial z_1 \partial z_2} & \cdots & \frac{\partial^2 c}{\partial z_1 \partial z_n} \\ \frac{\partial^2 c}{\partial z_1 \partial z_2} & \frac{\partial^2 c}{\partial z_2^2} & \cdots & \frac{\partial^2 c}{\partial z_2 \partial z_n} \\ \vdots & \vdots & \ddots & \vdots \\ \frac{\partial^2 c}{\partial z_1 \partial z_n} & \frac{\partial^2 c}{\partial z_2 \partial z_n} & \cdots & \frac{\partial^2 c}{\partial z_n^2} \end{bmatrix} = 2\mathbf{J}_h^T \mathbf{J}_h. \tag{6}$$

The bordered Hessian is a useful tool for determining the convexity of a problem when the Hessian is incapable of determining it (second-order tests are inconclusive). It is

$$\mathbf{BH} = \begin{bmatrix} 0 & \frac{\partial c}{\partial z_1} & \cdots & \frac{\partial c}{\partial z_n} \\ \frac{\partial c}{\partial z_1} & \frac{\partial^2 c}{\partial z_1^2} & \cdots & \frac{\partial^2 c}{\partial z_1 \partial z_n} \\ \vdots & \vdots & \ddots & \vdots \\ \frac{\partial c}{\partial z_n} & \frac{\partial^2 c}{\partial z_1 \partial z_n} & \cdots & \frac{\partial^2 c}{\partial z_n^2} \end{bmatrix} = \begin{bmatrix} 0 & \nabla c^T \\ \nabla c & \mathbf{H}_c \end{bmatrix}. \tag{7}$$

These definitions find significant use in section IV. Additional details regarding these tools can be found in [20].

This article has been accepted for publication in a future issue of this journal, but has not been fully edited. Content may change prior to final publication. Citation information: DOI 10.1109/TIE.2020.2982105, IEEE Transactions on Industrial Electronics

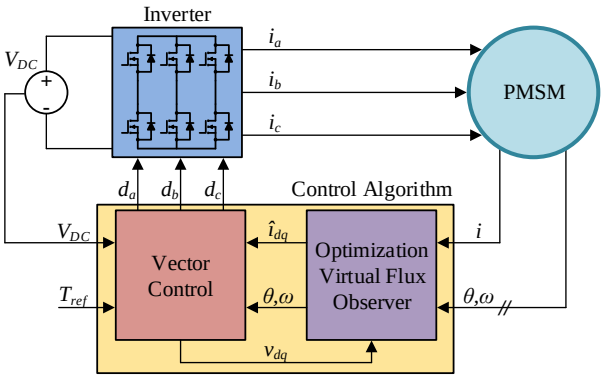

Fig. 1: System block diagram with the virtual flux observer.

III. Modelling

The system under study is presented in Fig. 1 and the designed observer is summarized in Fig. 2. This section describes the major components required to realize it.

Note that the model is defined with states λ_{dq}^{+} and λ_{dq}, i.e. next-step and current-step values, whereas the inputs to the cost function in Fig. 2 are λ_{dq} and λ_{dq}^{-}, i.e. current-step and previous-step values. The former owes to convention for discrete-time state-space systems and observers/estimators [21], [22]; the latter is a result of a physical system: a future measurement y^{+} cannot be realized. The two notations are equivalent, with the former used to conform with convention.

A. Coordinate System Transformations

To facilitate modelling and control implementation, as well as calculations, a series of transformations are made to change from time-varying sinusoids–which can be difficult to track and control–to constant (DC) quantities.

The first step in the coordinate system transformation process is to use the Clarke transform, which converts the three-phase system to an equivalent two-phase orthogonal system of sinusoids. It is performed as $x_{\alpha\beta} = \mathbf{T} x_{abc}$, where

$$\mathbf{T} = \frac{2}{3}\begin{bmatrix} 1 & -\frac{1}{2} & -\frac{1}{2} \\ 0 & \frac{\sqrt{3}}{2} & -\frac{\sqrt{3}}{2} \end{bmatrix}. \tag{8}$$

Still operating with sinusoids, it becomes necessary to apply a second transformation, the Park transform, to convert the two-phase system to an equivalent DC representation. It is achieved by multiplying the $\alpha\beta$ system with a rotational matrix that rotates at the same rate as the sinusoids, such that the quantities appear DC. This conversion is computed as $x_{dq} = \mathbf{P}(\theta)\, x_{\alpha\beta}$, where

$$\mathbf{P}(\theta) = \begin{bmatrix} \cos\theta & \sin\theta \\ -\sin\theta & \cos\theta \end{bmatrix}. \tag{9}$$

Because pulse width modulation (PWM) is enacted on a per-phase basis, it becomes necessary to reverse the process and convert back from dq to abc to generate the duty cycles that apply voltage. Reversing the Park transform is simple, as its transpose is its inverse; i.e. $\mathbf{P}^{-1}(\theta) = \mathbf{P}^{T}(\theta)$. The Clarke transform, however, requires more consideration as the matrix is not square. The inverse of a non-square matrix can be calculated by using the Moore-Penrose pseudoinverse [23], designated by the superscript †. Applying this operator to the Clarke transform $\mathbf{T}$ yields its pseudoinverse

$$\mathbf{T}^{\dagger} = \frac{3}{2}\begin{bmatrix} 1 & 0 \\ -\frac{1}{3} & \frac{\sqrt{3}}{3} \\ -\frac{1}{3} & -\frac{\sqrt{3}}{3} \end{bmatrix}. \tag{10}$$

An additional transformation is introduced, which is the so-called *sensor selection transform*. The purpose of this transformation is to determine what current sensors are present in the system. It is written as

$$\mathbf{Q} = \begin{bmatrix} phA & 0 & 0 \\ 0 & phB & 0 \\ 0 & 0 & phC \end{bmatrix}, \tag{11}$$

where phA, phB and $phC \in \{0,1\}$ and denote the absence (0) or presence (1) of a sensor.

When transforming directly from dq to abc with only one phase current sensor present, i.e. $i = \mathbf{Q}\mathbf{T}^{\dagger}\mathbf{P}^{-1}(\theta)\, i_{dq} = \mathbf{C}\mathbf{P}^{-1}(\theta)\, i_{dq}$, the process can be simplified to

$$\mathbf{C}\mathbf{P}^{-1}(\theta) = \left[\cos\left(\theta - k\tfrac{2\pi}{3}\right), \quad -\sin\left(\theta - k\tfrac{2\pi}{3}\right)\right], \tag{12}$$

where $k \in \{0,1,2\}$ and denotes what sensor is present. As a result, $k = 0$ means the phase A sensor is present, whereas $k = 2$ means phase C is.

B. Electric Machine Dynamical Model

The PMSM model is first introduced with flux as the states–known as virtual flux–and in the $\alpha\beta$ frame, both of which are used for problem generalization. Virtual flux has the benefit of providing a more generic problem formulation and, as a result, has found use in a wide variety of applications: PMSMs [5], [17]; switched reluctance machines [24]; and grid-tied inverters [25]. The model is converted to dq when appropriate to better mirror other current observers in literature [10]–[13].

The discrete-time $\alpha\beta$ flux model of a PMSM is realized by applying a first-order discretiziation to the continuous-time model defined in [17] and is written as

$$\lambda_{\alpha\beta}^{+} = \lambda_{\alpha\beta} + T_s\left(v_{\alpha\beta} - R i_{\alpha\beta}\right) = \lambda_{\alpha\beta} + T_s \bar{u}_{\alpha\beta} \tag{13a}$$

$$\theta^{+} = \theta + T_s\omega, \tag{13b}$$

where $v_{\alpha\beta}$, $i_{\alpha\beta}$ and $\bar{u}_{\alpha\beta}$ are the $\alpha\beta$ voltages, currents and compensated terminal voltages, respectively, applied to the PMSM; R is the per-phase stator resistance; θ and ω are the electrical position and speed, respectively, of the PMSM; and T_s is the sampling period.

The PMSM model (13) is given in flux, whereas the measurements available are in current ($y = i$, $y^{+} = i^{+}$). Conversion between current and flux can be achieved by way of the current-flux map of the machine $\mathcal{L}$ and its inverse $\mathcal{L}^{-1}$, performed as $\lambda_{\alpha\beta} = \mathcal{L}(i_{\alpha\beta})$ and $i_{\alpha\beta} = \mathcal{L}^{-1}(\lambda_{\alpha\beta})$, respectively. Typically, the mapping $\mathcal{L}$ is known in dq and not $\alpha\beta$, requiring an additional Park transformation within

This article has been accepted for publication in a future issue of this journal, but has not been fully edited. Content may change prior to final publication. Citation information: DOI 10.1109/TIE.2020.2982105, IEEE Transactions on Industrial Electronics

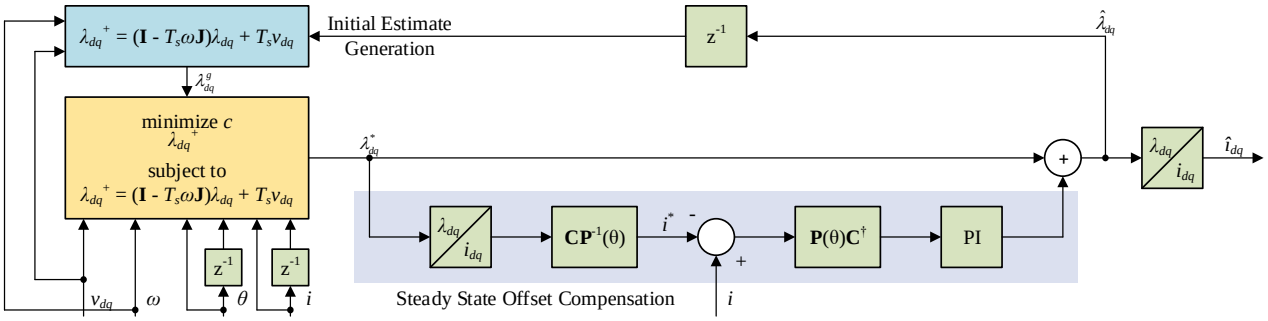

Fig. 2: Block diagram of the optimization-based virtual flux observer used in Fig. 1.

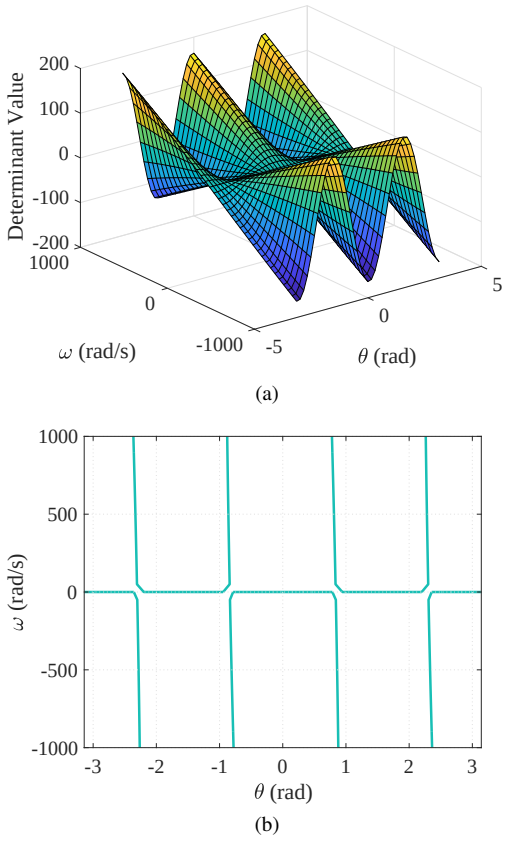

Fig. 3: The determinant of (a) the Jacobian $\mathbf{J}_h$ and (b) its zero-level set.

the current-flux map function, such that $\lambda_{dq} = \mathcal{L}\left(\mathbf{P}\left(\theta\right) i_{\alpha\beta}\right)$ and $i_{dq} = \mathcal{L}^{-1}\left(\mathbf{P}\left(\theta\right)\lambda_{\alpha\beta}\right)$. To convert from dq to $\alpha\beta$, an inverse Park transformation must be applied, i.e. $\lambda_{\alpha\beta} = \mathbf{P}^{-1}\left(\theta\right)\mathcal{L}\left(\mathbf{P}\left(\theta\right) i_{\alpha\beta}\right)$ and $i_{\alpha\beta} = \mathbf{P}^{-1}\left(\theta\right)\mathcal{L}^{-1}\left(\mathbf{P}\left(\theta\right)\lambda_{\alpha\beta}\right)$.

Substituting (13) into (2) with the aforementioned caveats gives the h function for the PMSM in $\alpha\beta$

$$h_{\alpha\beta}\left(i, i^{+}, \bar{u}_{\alpha\beta}, \hat{z}\right) = \begin{bmatrix} \lambda_{\alpha\beta} + T_s\bar{u}_{\alpha\beta} - \lambda_{\alpha\beta}^{+} \\ \mathbf{CP}^{-1}\left(\theta\right)\mathcal{L}^{-1}\left(\mathbf{P}\left(\theta\right)\hat{\lambda}_{\alpha\beta}\right) - i \\ \mathbf{CP}^{-1}\left(\theta^{+}\right)\mathcal{L}^{-1}\left(\mathbf{P}\left(\theta^{+}\right)\hat{\lambda}_{\alpha\beta}^{+}\right) - i^{+} \end{bmatrix}, \tag{14}$$

recalling the relationship with (2): $f\left(x, u, p\right)$ is the state equation of the PMSM in the $\alpha\beta$ frame and $g\left(x, p\right)$ is the output equation of the state-space system. Simplifying the transforms applied to the current-flux map per (12) yields $\mathbf{CP}^{-1}\left(\theta\right)\mathcal{L}^{-1}\left(\mathbf{P}\left(\theta\right)\hat{\lambda}_{\alpha\beta}\right) = \hat{\imath}$, such that $h_{\alpha\beta}$ is taking the difference $\hat{y} - y = \hat{\imath} - i$.

An adjustment must be made to the h function of (14) by noting a limitation of the observer when only one phase current sensor is available. The formulation as it stands requires precise knowledge of $x^{+} = \lambda_{\alpha\beta}^{+}$, which can only be known to such a degree when at least two sensors are available. Hence, it becomes challenging to meaningfully minimize the difference $f\left(x, u, p\right) - x^{+}$. Therefore, it is useful to shift this equation from the cost function explicitly to being a constraint on the problem; i.e. it is mandated that $x^{+} = f\left(x, u, p\right)$, changing the optimization problem to

$$z^{*} = \begin{array}{ll} \underset{\hat{z}}{\text{minimize}} & \bar{h}_{\alpha\beta}\left(i, i^{+}, \bar{u}_{\alpha\beta}, \hat{z}\right)^{T}\mathbf{N}\bar{h}_{\alpha\beta}\left(i, i^{+}, \bar{u}_{\alpha\beta}, \hat{z}\right) \\ \text{subject to} & \hat{\lambda}_{\alpha\beta}^{+} = \hat{\lambda}_{\alpha\beta} + T_s\bar{u}_{\alpha\beta} \end{array} \tag{15}$$

where $h_{\alpha\beta}$ has been modified to $\bar{h}_{\alpha\beta}$, which is defined as

$$\bar{h}_{\alpha\beta}\left(i, i^{+}, \bar{u}_{\alpha\beta}, \hat{z}\right) = \begin{bmatrix} \mathbf{CP}^{-1}\left(\theta\right)\mathcal{L}^{-1}\left(\mathbf{P}\left(\theta\right)\hat{\lambda}_{\alpha\beta}\right) - i \\ \mathbf{CP}^{-1}\left(\theta^{+}\right)\mathcal{L}^{-1}\left(\mathbf{P}\left(\theta^{+}\right)\hat{\lambda}_{\alpha\beta}^{+}\right) - i^{+} \end{bmatrix}. \tag{16}$$

As a result of this adjustment, $\mathbf{N} \in \mathbb{R}^{(m+2r)\times(m+2r)} \rightarrow \mathbf{N} \in \mathbb{R}^{2r\times 2r}$ and $h \in \mathbb{R}^{(m+2r)\times 1} \rightarrow h \in \mathbb{R}^{2r\times 1}$.

For commonality with other phase current observers [10]–[13], a change to the dq model is made by recalling that $\lambda_{dq} = \mathbf{P}\left(\theta\right)\lambda_{\alpha\beta}$. Furthermore, a simplification is made by changing to a linear model by making the assumption that saturation does not occur and that the flux is linearly proportional to the current in the stator windings; i.e. the current-flux map is

$$\lambda_{dq} = \mathcal{L}\left(i_{dq}\right) \approx \mathbf{L}_{dq} i_{dq} + \psi_{dq}, \tag{17}$$

with $\mathbf{L}_{dq} = \text{diag}\left(\left[L_d, L_q\right]\right)$, a diagonal matrix of the d- and q-axis inductances, respectively, of the machine; and ψ_{dq}, the dq flux of the permanent magnets, where $\psi_{dq} = \left[\psi, 0\right]^{T}$.

The optimization-based observer is general enough to be applied to the nonlinear model and, indeed, it is in [5]; however, it is prudent to examine the linear model first to

This article has been accepted for publication in a future issue of this journal, but has not been fully edited. Content may change prior to final publication. Citation information: DOI 10.1109/TIE.2020.2982105, IEEE Transactions on Industrial Electronics

assess concept feasibility. Applying both the change to the dq model and the linearization of (17) changes (16) to

$$\bar{h}_{dq}\left(i, i^{+}, \bar{u}_{dq}, \hat{z}\right)=\begin{bmatrix}\mathbf{C}\mathbf{P}^{-1}\left(\theta\right)\mathbf{L}_{dq}^{-1}\left(\hat{\lambda}_{dq}-\psi_{dq}\right)-i\\ \mathbf{C}\mathbf{P}^{-1}\left(\theta^{+}\right)\mathbf{L}_{dq}^{-1}\left(\hat{\lambda}_{dq}^{+}-\psi_{dq}\right)-i^{+}\end{bmatrix}, \tag{18}$$

where $\hat{\lambda}_{dq}^{+}=\left(\mathbf{I}-T_s\omega\mathbf{J}\right)\hat{\lambda}_{dq}+T_s v_{dq}-T_s R\hat{\imath}_{dq}$, resulting from the discretization and transformation of $\dot{\lambda}_{\alpha\beta}$ to $\dot{\lambda}_{dq}$, and $\mathbf{J}=\left[[0,1]^T,[-1,0]^T\right]$, which accounts for cross-coupling effects between the two axes in the dq frame. In an attempt to simplify the problem, $R\hat{\imath}_{dq}$ is assumed to be small enough to neglect, allowing for the removal of an additional nested $\hat{\lambda}_{dq}$ term from the formulation.

With the formulation finalized in dq, it is beneficial to present how (2) became (18) by specifiying what the initial, generic variables are, as well as the size of each vector in the system. For the PMSM drive system, there are two states and two next-step states ($m=2$), the dq fluxes, $x=\hat{\lambda}_{dq}=\left[\hat{\lambda}_d,\quad \hat{\lambda}_q\right]^T$ and $x^{+}=\hat{\lambda}_{dq}^{+}=\left[\hat{\lambda}_d^{+},\quad \hat{\lambda}_q^{+}\right]^T$, respectively; four parameters ($p=4$), $p=\left[L_d,\quad L_q,\quad R,\quad \psi\right]^T$; two inputs ($n=2$), the dq voltages, $u=v_{dq}=\left[v_d,\quad v_q\right]^T$; and one output ($r=1$), the measured current $y=i$ and the next-step measurement $y^{+}=i^{+}$. Because only one phase current is measured every T_s, $h\in\mathbb{R}^{2\times 1}$, making $\mathbf{N}\in\mathbb{R}^{2\times 2}$.

The mechanical equations for the system are neglected in the modelling of the observer, save for noting in (13) the relationship between position and speed, as a consequence of the linearization of the system. This linearization is achieved by assuming that the mechanical time constant is much larger than the electrical one and is commonly made for current observers [10]–[13] and automotive systems in general, where intertia is large due to the vehicle's mass.

Many systems define a reference torque, T_{ref}, that determines the dq currents to be used in the field-oriented control algorithm given a desired operating point. The electromagnetic torque equation can be used to determine these currents. In the dq frame, it is written as

$$T_e=\frac{3}{2}p_p\left(\psi i_q+\left(L_d-L_q\right)i_d i_q\right), \tag{19}$$

where p_p is the number of pole pairs in the electric machine.

C. Cost Function

The cost function is the same as described in section II and is given in (3). It can be built for the problem at hand by substituting for h with (18).

The addition of a so-called filter term, introduced in [3], can be used to help the problem in two ways: 1) it penalizes large changes from the expected estimate; and 2) it adds a convex term to the problem, which can help with solving a poorly conditioned, albeit convex, system. The modified cost function is written as

$$\bar{c}=h^T\mathbf{N}h+\rho\left\|\hat{\lambda}_{dq}^{+}-\lambda_{dq}^{g}\right\|_2^2, \tag{20}$$

where ρ is a non-negative number and λ_{dq}^{g} is the initial guess of the dq flux given by the state-space model, calculated as $\lambda_{dq}^{g}=\left(\mathbf{I}-T_s\omega\mathbf{J}\right)\hat{\lambda}_{dq}+T_s v_{dq}$, which is a constant value during the optimization and is updated every sampling period.

The filter term's significance is that it suggests the neighbourhood of the optimal flux λ_{dq}^{*} to the estimator via the initial estimate λ_{dq}^{g}. How much the observer relies on this initial estimate depends on the value of ρ: if ρ is large, then it will rely significantly on λ_{dq}^{g}; if ρ is small, then the observer will start in the neighbourhood of λ_{dq}^{g} but will be permitted to find a different flux; and if ρ is zero, the estimate relies exclusively on the model of the system, which is the cost function (3).

The filter term can also be thought of as a limit on how quickly the estimated flux that will be applied to the system is allowed to change. With a large ρ, the estimated flux is stipulated to be close to the initial guess and will change at roughly the same rate as that guess (i.e. behaves like a linear observer). If ρ is small, then a larger difference is permitted as the optimizer searches for what it believes is the true flux, enabling more rapid changes in value.

D. Steady State Offset Compensation

In a practical system, the system's parameters are often specified within a tolerance band and can change even more

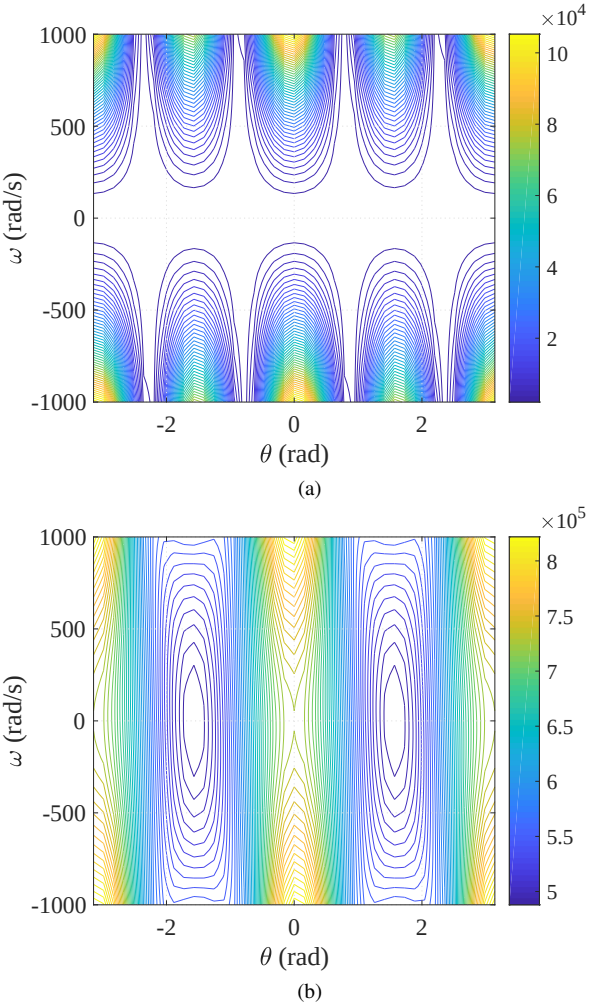

Fig. 4: The contours of $\det\mathbf{H}_{\bar{c}}$ with filter term (a) $\rho=0$ and (b) $\rho=10$. The system is strictly convex with $\rho>0$.

This article has been accepted for publication in a future issue of this journal, but has not been fully edited. Content may change prior to final publication. Citation information: DOI 10.1109/TIE.2020.2982105, IEEE Transactions on Industrial Electronics

during operation; for example, as the motor heats up. In lieu of a detailed model, an integrator term has been added to the observer, whose purpose it is to compensate for modelling errors. The compensator follows the same structure as the one described in [13]: the estimated dq currents are converted to their three-phase equivalents and only the one being compared with the measurement is retained via $\hat{\imath} = \mathbf{C}\mathbf{P}^{-1}(\theta)\,\hat{\imath}_{dq}$. Then, the difference between measurement and estimate is taken, giving the error signal $e = i - \hat{\imath}$, which is converted to dq via the incomplete transformation $e_{dq} = \left(\mathbf{C}\mathbf{P}^{-1}(\theta)\right)^{\dagger} e = \mathbf{P}(\theta)\,\mathbf{C}^{\dagger} e$ and fed to the proportional-integral (PI) compensator, generating the compensation signal. As a result of the incomplete abc to dq transformation, sinusoidal oscillations at two times the fundamental frequency are injected into the estimate. If the error is small, then these oscillations will also be small.

A major benefit of using a PI compensator to perform steady state error compensation is that a detailed current-flux map of a machine is not necessary, which is beneficial for industrial applications where a machine is not extensively characterized and nameplate parameters are primarily employed. For applications where the machine is known well and a detailed current-flux map is known, then the PI compensator could be omitted and the steady state oscillations it injects avoided.

IV. Identifiability and Convexity Analyses

Identifiability and convexity are first studied for the base case of the system, i.e. with no filter term added ($\rho = 0$). Once the observer is understood in full via Theorems 1 through 4, the filter term is added ($\rho > 0$) to augment the cost function, with the benefit presented in Theorem 5.

A. Identifiability

Identifiability is the property that the parameters of a system can be uniquely estimated from inputs and measurements. In this work, identifiability is used to estimate the states of the system, with this change in goal achieved by taking two adjacent samples, y and y^{+}, and treating them like parameters via the state-parameter vector z.

Identifiability and observability are similar concepts, where being observable means that a unique set of states can be determined from the inputs and outputs of the system. Given their similarity, it should be expected that the conditions for unique estimation should be similar, which are shown and compared with [13] in Theorem 1 and Corollary 1.

A system is identifiable when the Jacobian is full *column* rank [26]–[28]. With this information in hand, it is possible to determine whether the optimization-based virtual flux observer is identifiable when only one phase current sensor is present by studying $\bar{h}_{dq}$, as given in (18).

Theorem 1. *Let a motor drive have one current sensor on phase $k \in \{0,1,2\}$. The system is identifiable if and only if $\omega \neq 0$ and*

$$\frac{c_{\Sigma\Delta}\cos\left(T_s\omega+\alpha\right) - 2L_{\Sigma}L_{\Delta}T_s\omega\cos\left(2\theta - k\frac{4\pi}{3} + T_s\omega\right)}{\left(L_{\Sigma}^2 - L_{\Delta}^2\right)\left(T_s^2\omega^2+1\right)} \neq 0,$$

with $L_{\Delta} = \frac{1}{2}\left(L_d - L_q\right)$ and $L_{\Sigma} = \frac{1}{2}\left(L_d + L_q\right)$.

Proof. The Jacobian $\mathbf{J}_h$ is full rank if and only if $\det \mathbf{J}_h \neq 0$, where $\det \mathbf{J}_h =$

$$\frac{c_{dq}\cos\left(T_s\omega+\alpha\right) - \left(L_d^2 - L_q^2\right)T_s\omega\cos\left(2\theta - k\frac{4\pi}{3} + T_s\omega\right)}{2L_d^2L_q^2\left(T_s^2\omega^2+1\right)}.$$

Equivalence between statements can be shown by applying the following identities to $\det \mathbf{J}_h$: $L_d^2 + L_q^2 = 2\left(L_{\Sigma}^2 + L_{\Delta}^2\right)$, $L_d^2 - L_q^2 = 4L_{\Sigma}L_{\Delta}$ and $L_dL_q = \left(L_{\Sigma}^2 - L_{\Delta}^2\right)$. Furthermore, the trigonometric identity $a\cos(x) - b\sin(x) = c\cos(x+\alpha)$ is employed, where $c = \sqrt{a^2+b^2}$ and $\alpha = \arctan\left(\frac{b}{a}\right)$. The dq terms are $a_{dq} = \left(L_d^2 + L_q^2\right)T_s\omega$ and $b_{dq} = 2L_dL_q$. Making the appropriate substitutions and employing once more the same trigonometric identity, it can be shown that the $\Sigma\Delta$ terms are $a_{\Sigma\Delta} = \left(L_{\Sigma}^2 + L_{\Delta}^2\right)T_s\omega$ and $b_{\Sigma\Delta} = \left(L_{\Sigma}^2 - L_{\Delta}^2\right)$. Note that the denominator is irrelevant, as the term $L_d^2L_q^2\left(T_s^2\omega^2+1\right) = \left(L_{\Sigma}^2 - L_{\Delta}^2\right)^2\left(T_s^2\omega^2+1\right)$ is always non-zero; therefore, it does not impact the determinant being equal to zero. ■

A major difference between this work and that of [13] is that the optimization-based virtual flux observer *does not require anisotropy* $(L_d \neq L_q)$ for estimation. Since excessive saturation of a PMSM can lead to isotropy $(L_d = L_q)$, this becomes an attractive property of the method; however, the tradeoff is that zero-speed operation becomes an issue. This limitation can be overcome by use of signal injection, as in [3] and [5], or by adding the filter term ρ to obtain the cost function (20). The latter approach is discussed in Theorem 5.

Corollary 1. *With one current sensor present and $\omega \neq 0$, the system is non-identifiable four times over a 2π period.*

Proof. This can be shown by setting $\det \mathbf{J}_h = 0$ and solving for θ. Doing so yields the four non-identifiable positions

$$\theta_1 = \frac{1}{2}\left(\arccos(x) + k\frac{4\pi}{3} - T_s\omega\right) \tag{21a}$$

$$\theta_2 = \theta_1 + \pi \tag{21b}$$

$$\theta_3 = \frac{1}{2}\left(2\pi - \arccos(x) + k\frac{4\pi}{3} - T_s\omega\right) \tag{21c}$$

$$\theta_4 = \theta_3 + \pi, \tag{21d}$$

where $x = c_{\Sigma\Delta}\cos\left(T_s\omega+\alpha\right)\left(2L_{\Sigma}L_{\Delta}T_s\omega\right)^{-1}$, with the same substitutions for $a_{\Sigma\Delta}$, $b_{\Sigma\Delta}$, $c_{\Sigma\Delta}$ and α as in Theorem 1. ■

The result of Corollary 1 can be plotted as well and is shown in Fig. 3. There is a striking resemblance between the determinant and zero-level set of the Jacobian and the observability matrix $\mathbf{O}$ shown in [13]. When comparing the non-observable and non-identifiable positions, both methods return near-identical values. These similarities give credence to the equivalency of the methods for phase current estimation.

B. Convexity

Having shown that the formulation is identifiable under certain conditions, it next becomes necessary to evaluate whether the system is convex, quasiconvex or non-convex. Convexity, or the lack thereof, is important for not only being able to find a unique set of states that satisfy the system, but also for being able to efficiently solve for the minima.

This article has been accepted for publication in a future issue of this journal, but has not been fully edited. Content may change prior to final publication. Citation information: DOI 10.1109/TIE.2020.2982105, IEEE Transactions on Industrial Electronics

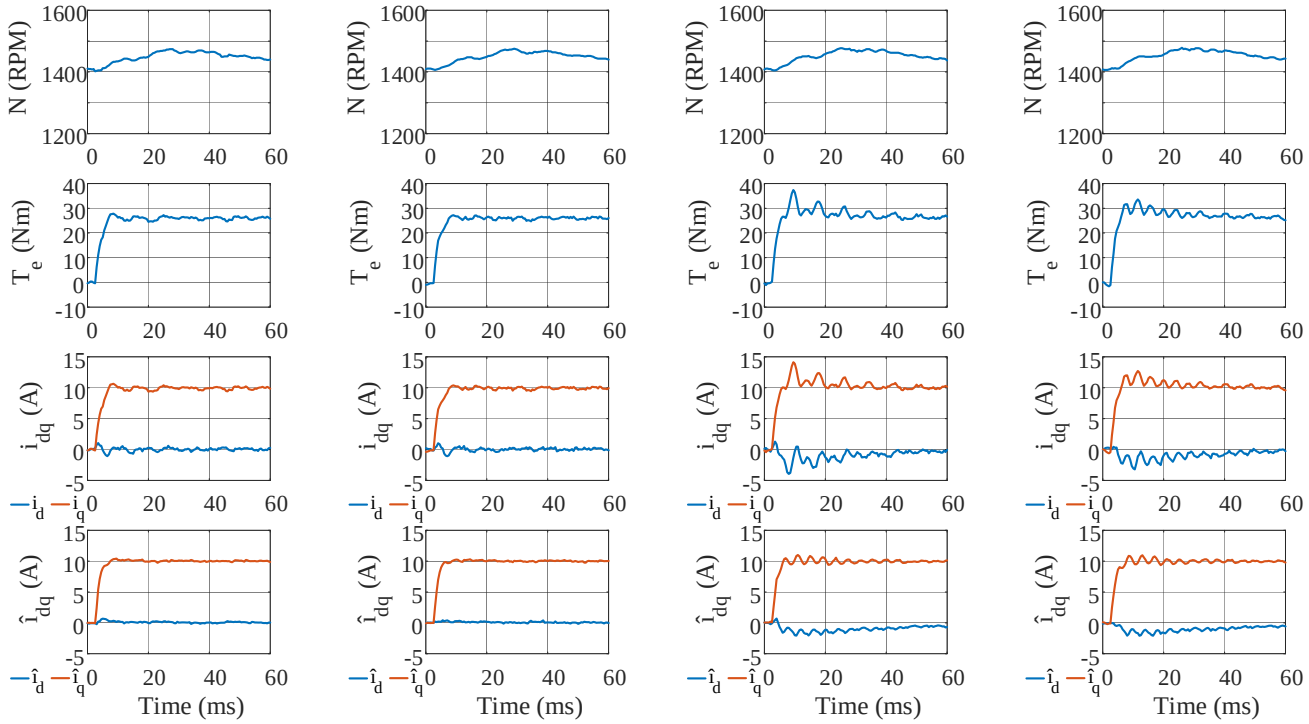

Fig. 5: Torque step ($i_q = 0A \rightarrow i_q = +10A$, $i_d = 0A$ at $t = 2.5$ms) experimental validation with (a) no observer parameter error, $\rho = 10$; (b) no observer parameter error, $\rho = 0.01$; (c) observer parameter error; $\rho = 10$; and (d) observer parameter error, $\rho = 0.01$. Shown are the mechanical speed (N), electromagnetic torque (T_e), measured dq currents (i_{dq}) and estimated dq currents ($\hat{i}_{dq}$).

Convexity is shown by first studying the cost function (3), i.e. $\rho = 0$, before proceeding to make $\rho > 0$ and using (20).

Theorem 2. *Let a motor drive have one current sensor on phase $k \in \{0,1,2\}$. The system is always positive semi-definite.*

Proof. The Hessian is defined as (6). It can be shown that, for any vector x, the following holds: $x^T \mathbf{H}_c x = 2x^T \mathbf{J}_h^T \mathbf{J}_h x \geq 0$; hence, the system is always positive semi-definite. ■

The system being positive semi-definite with respect to the Hessian means that it is not possible to tell whether the function is convex or not, as $\det \mathbf{H}_c = 0$ means that the second derivative test of the function is inconclusive. *Strict* convexity is when the Hessian is positive definite and guarantees that a unique global minimum can be found. Theorem 3 discusses the necessary conditions for strict convexity.

Theorem 3. *Let a motor drive have one current sensor on phase $k \in \{0,1,2\}$. The system is strictly convex when $\omega \neq 0$ and the electrical position is not one of those listed in* (21)*.*

Proof. Because $\mathbf{H}_c = 2\mathbf{J}_h^T \mathbf{J}_h$, it follows that, when $\det \mathbf{J}_h = 0$, $\det \mathbf{H}_c = 0$. Thus, when $\omega = 0$ or when the position is one of those listed in (21), $\det \mathbf{J}_h = \det \mathbf{H}_c = 0$ and the system is not strictly convex. Thus, $\omega \neq 0$ and $\theta \neq$ (21) result in $\det \mathbf{H}_c > 0$, meaning the system is strictly convex. ■

The other case arising from the Hessian being positive semi-definite is when $\det \mathbf{H}_c = 0$. Because the second derivative test fails, alternative approaches must be used to determine the convexity of the system. Theorem 4 discusses the details.

Theorem 4. *Let a motor drive have one current sensor on phase $k \in \{0,1,2\}$. The system is quasiconvex when $\omega = 0$ or $\theta =$ (21) (i.e. $\det \mathbf{H}_c = 0$).*

Proof. This can be shown by employing the bordered Hessian, defined in (7). When all leading principal minors $D_k \leq 0$, the system is quasiconvex. The first and third leading principal minors, i.e. D_1 and D_3, are both always zero; the second is $D_2 = -\frac{\partial c}{\partial z_1}\frac{\partial c}{\partial z_1} = -\left(\frac{\partial c}{\partial z_1}\right)^2 \leq 0$. Thus, all three leading principal minors are ≤ 0 and the system is quasiconvex. ■

Quasiconvexity is a beneficial property to have as it means the domain and its sublevel sets are convex. What this implies is that the function may not be globally convex, but it is convex within the region of operation and a minimum can be found.

Note that the system can be made strictly convex without restrictions by adding the filter term and using the cost function (20). Through this modification, the observer is capable of uniquely estimating the states $\hat{\lambda}_{dq}$ without restrictions, which is a significant departure from the linear observer of [13]. This point is elaborated upon in Theorem 5.

Theorem 5. *Let a motor drive have one current sensor on phase $k \in \{0,1,2\}$. The system is always strictly convex when*

This article has been accepted for publication in a future issue of this journal, but has not been fully edited. Content may change prior to final publication. Citation information: DOI 10.1109/TIE.2020.2982105, IEEE Transactions on Industrial Electronics

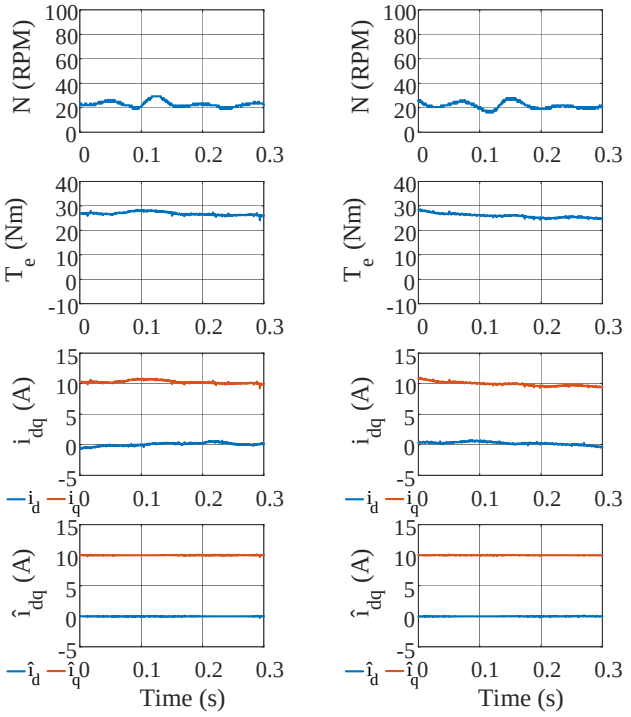

(a) (b)

Fig. 6: Low ($N = 20RPM \approx 1\%$ rated) speed steady state experimental validation with (a) no observer parameter error and (b) observer parameter error at $i_d = 0A$, $i_q = +10A$ and $\rho = 10$. Shown are the mechanical speed (N), electromagnetic torque (T_e), measured dq currents (i_{dq}) and estimated dq currents ($\hat{\imath}_{dq}$).

employing the cost function of (20)*, i.e. the filter term is added.*

Proof. Because the system under study is linear, the Hessian can be taken with respect to each component of the cost function; i.e. $\mathbf{H}_{\bar{c}} = \mathbf{H}_c + \mathbf{H}_\rho$, where $\mathbf{H}_c$ is the Hessian of the original cost function (3) and $\mathbf{H}_\rho$ is the Hessian of only the filter term. The sum of convex functions is convex [29]; hence, since $\mathbf{H}_\rho$ is always convex, the resulting sum is convex and the problem becomes always strictly convex. ■

Theorem 5 can also be shown graphically by plotting the contours of the determinant of the Hessian of the basic cost function (3) and the modified cost function (20), as in Fig. 4 With $\rho > 0$, strict convexity becomes apparent.

In augmenting the cost function with the filter term, the system is made strictly convex and all constraints on estimation eliminated. This changes the identifiability conditions previously derived, as discussed in Corollary 2.

Corollary 2. *The addition of the filter term to the cost function makes the system always identifiable.*

Proof. This follows from the definition of the Hessian, where $\mathbf{H}_c = 2\mathbf{J}_h^T\mathbf{J}_h$. Taking the determinant of this gives $\det \mathbf{H}_c = \det\left(2\mathbf{J}_h^T\mathbf{J}_h\right) = 2\det\mathbf{J}_h^T \det\mathbf{J}_h$. Since $\det\mathbf{H}_{\bar{c}} \neq 0$, $\det\mathbf{J}_h \neq 0$ and the system is always identifiable. ■

V. Optimization Problem Solution Implementation

In having shown the problem to be identifiable, the feasibility of pursuing an optimization-based approach has been demonstrated. Furthermore, by showing that the problem is strictly convex with the added filter term, it has been proven that the unique minima can be efficiently found without restriction. Therefore, in implementing a solution methodology, it becomes unnecessary to use more than a simple algorithm, such as Newton's method. The basic Newton step is given by

$$x_{k+1} = x_k - \gamma \mathbf{H}_c^{-1} \nabla c\left(x_k\right), \tag{22}$$

where γ is a multiplier used to fine-tune the size of the taken step, which has an optimal value of the inverse of the maximum eigenvalue of $\mathbf{H}_c$. At the end of each iteration, the relative error between x_{k+1} and x_k is assessed to determine whether a solution has been found. This is performed as

$$\left\| \frac{x_{k+1} - x_k}{x_k} \right\|_2^2 \leq \epsilon, \tag{23}$$

where ϵ is an error threshold defined as being acceptable for the application. In practice, only a few iterations are required to reach this condition and terminate the search.

VI. Experiments

The optimization-based virtual flux observer has been experimentally validated on a three-phase PMSM with parameters as in Table I. The PMSM is connected to an induction machine in a dynamometer configuration, as shown in Fig. 8. Experimental validation entailed high and low speed torque control and speed control with the observer providing the currents to the field-oriented control algorithm.

TABLE I: PMSM parameters.

Parameter	Nominal Quantity	Introduced Error
Pole pairs (p_p)	5	-
Stator resistance (R)	0.4Ω	-100%
d-axis inductance (L_d)	10.5mH	+20%
q-axis inductance (L_q)	12.9mH	+40%
Permanent magnet flux (ψ)	0.3491Wb	+10%

High speed torque control involved applying a current (torque) step, bringing the PMSM from $i_q = 0A$ to $i_q = +10A$ with $i_d = 0A$ ($T_e = 26Nm$) at a mechanical speed of $N = 1400RPM$ (set by the induction machine) and a DC-link voltage of $V_{DC} = 700V$. The steps were undertaken with and without parameter error and with filter parameter $\rho = 10$ and $\rho = 0.01$, the results of which are shown in Fig. 5. The PMSM quickly reached the steady state with minimal overshoot in all cases, even with extreme parameter error. Steady state current ripple is comparable to the linear observer of [13], given in Table II. The optimization-based observer exhibits superior transient response, with less ringing after the torque step.

Low speed operation was realized by applying maximum torque ($T_e = 26Nm$ with $i_q = +10A$ and $i_d = 0A$) while rotating at $N = 20RPM$, which is approximately 1% of rated speed (1800RPM). Like at high speed, the PMSM is controlled well with the estimated dq currents, as shown in Fig. 6.

This article has been accepted for publication in a future issue of this journal, but has not been fully edited. Content may change prior to final publication. Citation information: DOI 10.1109/TIE.2020.2982105, IEEE Transactions on Industrial Electronics

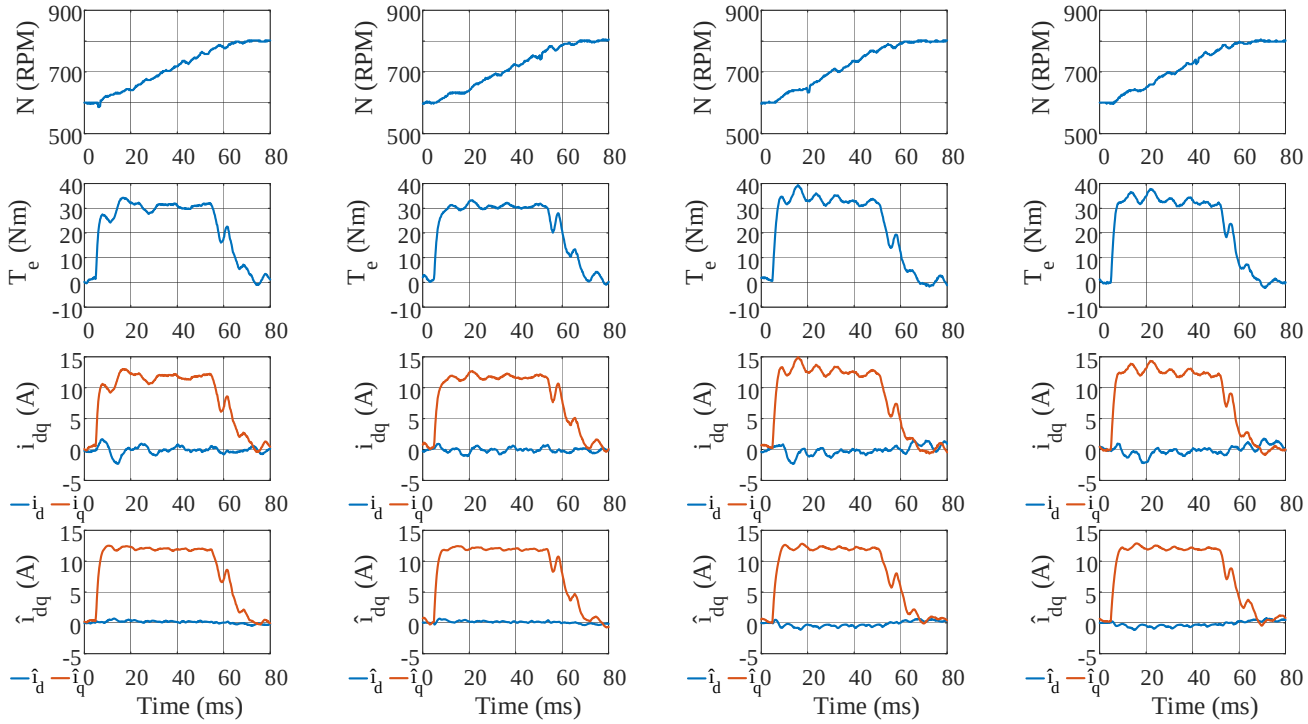

Fig. 7: Speed step ($N = 600RPM \rightarrow N = 800RPM$ at $t = 5.0$ms) experimental validation with (a) no observer parameter error, $\rho = 10$; (b) no observer parameter error, $\rho = 0.01$; (c) observer parameter error; $\rho = 10$; and (d) observer parameter error, $\rho = 0.01$. Shown are the mechanical speed (N), electromagnetic torque (T_e), measured dq currents (i_{dq}) and estimated dq currents ($\hat{i}_{dq}$).

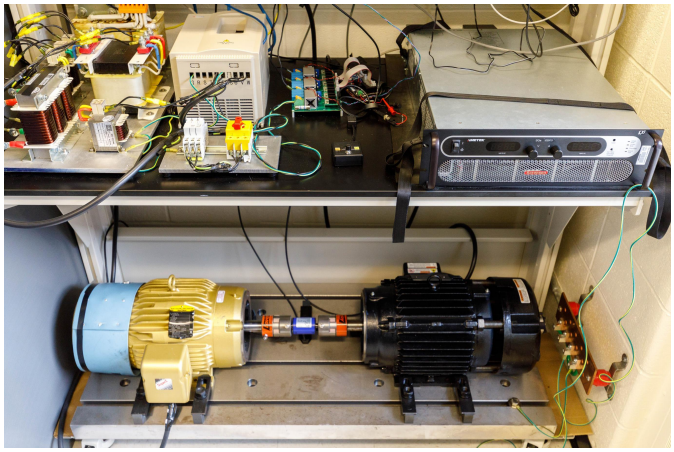

Fig. 8: The experimental setup.

Speed control is another important operating mode for automotive and industrial applications. To show this, a speed step was commanded, taking the PMSM from $N = 600RPM$ to $N = 800RPM$, with and without parameter error and with $\rho = 10$ and $\rho = 0.01$, the results of which are given in Fig. 7. The system is controlled well with the estimated currents, even with extreme observer parameter error. Like in the torque control case, the system was controlled well with the observer.

The ρ parameter is a degree of freedom available in the design process of the optimization-based observer, determining how much trust is placed in the initial estimate provided to the estimator. A large value of ρ places high trust in the initial estimate, with the optimization process acting more as a refinement of the guess; a small value of ρ places low trust in the initial estimate, suggesting the neighbourhood of the optimal flux that the optimizer then searches over. The impact of high and low ρ are shown in Figs. 5 and 7, as well as in Table II. Together, they show that ρ primarily impacts transient operation with minimal influence on the steady state. A low value of ρ positively benefits both torque and speed transients, helping to smooth the response and reduce peak currents, both of which are most visible in the former case, with slight benefit to the latter. In the steady state, the RMS current ripple is very similar for both values of ρ that were tested.

TABLE II: Comparison of observer RMS current ripple with varying parameter error at $N = 1400$RPM.

Parameter Case	Observer		
	Optimization, $\rho = 10$	Optimization, $\rho = 0.01$	Linear [13]
Table I Nominal	0.271	0.251	0.279
$0.8L_d$	0.237	0.216	0.275
$1.2L_d$	0.340	0.304	0.275
$0.6L_q$	0.289	0.392	0.275
$1.4L_q$	0.233	0.232	0.275
0.9ψ	0.305	0.286	0.275
1.1ψ	0.304	0.286	0.275
Table I Error	0.272	0.277	0.266

In terms of computational effort, the optimization-based virtual flux observer requires approximately 1000 clock cycles per iteration (about 5μs) with an error threshold $\epsilon = 0.1$ on the 32-bit, 200MHz DSP being used. This is higher than the 300 clock cycles (1.5μs) required for the linear observer [13]; however, this increase may be acceptable, given the wider applicability, reduced ringing after transients and greater design flexibility the method affords.

VII. Conclusion

This paper presented an optimization-based virtual flux observer that can accurately estimate the three-phase currents of a PMSM with only one phase current measurement. While similar in nature to the work presented in [13], the proposed method extends the range of permanent magnet machines that a one sensor observer can be used with by eliminating the need for machine anisotropy. By augmenting the cost function with a so-called filter term, all estimation constraints are eliminated. Experiments demonstrate the equivalency of the two methods in the steady state; however, the optimization-based observer exhibits reduced ringing after transients. Design flexibility is enhanced through the ability to tune the filter parameter ρ and, with higher bandwidth relative to the linear observer, greater response tuning of the field-oriented control algorithm is possible. The sole drawback of the method is an increase in computational time of several microseconds.

References

[1] B. Bilgin *et al.*, "Making the Case for Electrified Transportation," *IEEE Trans. Transport. Electrific.*, vol. 1, no. 1, pp. 4–17, 2015.

[2] B. Nahid-Mobarakeh, F. Meibody-Tabar, and F.-M. Sargos, "Back EMF estimation-based sensorless control of PMSM: Robustness with respect to measurement errors and inverter irregularities," *IEEE Trans. Ind. Appl.*, vol. 43, no. 2, pp. 485–494, 2007.

[3] Y. Sun *et al.*, "Unified Wide-Speed Sensorless Scheme Using Nonlinear Optimization for IPMSM Drives," *IEEE Trans. Power Electron.*, vol. 32, no. 8, pp. 6308–6322, 2016.

[4] F. Toso, D. Da Ru, and S. Bolognani, "A moving horizon estimator for the speed and rotor position of a sensorless PMSM Drive," *IEEE Trans. Power Electron.*, vol. 34, no. 1, pp. 580–587, 2019.

[5] X. Yong and M. Preindl, "Optimization-based position estimation of pm synchronous machine motor drives with magnetic saturation," in *SLED*, 2018, pp. 1–6.

[6] M. Carpaneto *et al.*, "Dynamic performance evaluation of sensorless permanent-magnet synchronous motor drives with reduced current sensors," *IEEE Trans. Ind. Electron.*, vol. 59, no. 12, pp. 4579–4589, 2012.

[7] J. I. Ha, "Current prediction in vector-controlled PWM inverters using single DC-link current sensor," *IEEE Trans. Ind. Electron.*, vol. 57, no. 2, pp. 716–726, 2010.

[8] H. Ye and A. Emadi, "A six-phase current reconstruction scheme for dual traction inverters in hybrid electric vehicles with a single dc-link current sensor," *IEEE Trans. Veh. Technol.*, vol. 63, no. 7, pp. 3085–3093, 2014.

[9] Y. Cho, T. LaBella, and J.-S. Lai, "A three-phase current reconstruction strategy with online current offset compensation using a single current sensor," *IEEE Trans. Ind. Electron.*, vol. 59, no. 7, pp. 2924–2933, 2012.

[10] Y.-s. Jeong *et al.*, "Fault detection and fault-tolerant control of interior permanent-magnet motor drive system for electric vehicle," *IEEE Trans. Ind. Appl.*, vol. 41, no. 1, pp. 46–51, 2005.

[11] G. H. B. Foo, X. Zhang, and D. M. Vilathgamuwa, "A sensor fault detection and isolation method in interior permanent-magnet synchronous motor drives based on an extended kalman filter," *IEEE Trans. Ind. Electron.*, vol. 60, no. 8, pp. 3485–3495, 2013.

[12] G. F. H. Beng, X. Zhang, and D. M. Vilathgamuwa, "Sensor fault-resilient control of interior permanent-magnet synchronous motor drives," *IEEE/ASME Trans. Mechatronics*, vol. 20, no. 2, pp. 855–864, 2015.

[13] M. Eull *et al.*, "A Current Observer to Reduce the Sensor Count in Three-Phase PM Synchronous Machine Drives," *IEEE Trans. Ind. Appl.*, vol. 55, no. 5, pp. 4780–4789, 2019.

[14] A. Corne *et al.*, "Nonlinear Estimation of Stator Currents in a Wound Rotor Synchronous Machine," *IEEE Trans. Ind. Appl.*, vol. 54, no. 4, pp. 3858–3867, 2018.

[15] S. Morimoto, M. Sanada, and Y. Takeda, "High-performance current-sensorless drive for PMSM and SynRM with only low-resolution position sensor," *IEEE Trans. Ind. Appl.*, vol. 39, no. 3, pp. 792–801, 2003.

[16] LEM, "LF series for current measurement from 200 A up to 2000 A nominal," Tech. Rep. [Online]. Available: https://www.lem.com/images/stories/files/Products/P1_5_1_industry/E_CH22102_2104.pdf

[17] M. Preindl, "Robust Control Invariant Sets and Lyapunov-Based MPC for IPM Synchronous Motor Drives," *IEEE Trans. Ind. Electron.*, vol. 63, no. 6, pp. 3925–3933, 2016.

[18] S. Nalakath, M. Preindl, and A. Emadi, "Online multi-parameter estimation of interior permanent magnet motor drives with finite control set model predictive control," *IET Electr. Power Appl.*, vol. 11, no. 5, pp. 944–951, 2017.

[19] L. Tarisciotti *et al.*, "A Distributed Model Predictive Control Strategy for Back-to-Back Converters," *IEEE Trans. Ind. Electron.*, vol. 63, no. 9, pp. 5867–5878, 2016.

[20] G. Giorgi, A. Guerraggio, and J. Thierfelder, *Mathematics of Optimization: Smooth and Nonsmooth Case*, 1st ed. Elsevier Science, 2004.

[21] R. E. Kalman, "A new approach to linear filtering and prediction problems," *Journal of Basic Engineering*, vol. 82, no. 1, pp. 35–45, 1960.

[22] E. Tse and M. Athans, "Optimal Minimal-Order Observer-Estimators for Discrete Linear Time-Varying Systems," *IEEE Trans. Autom. Control*, vol. 15, no. 4, pp. 416–426, 1970.

[23] C.-T. Chen, *Linear System Theory and Design*, 3rd ed. New York: Oxford University Press, 1999.

[24] D. F. Valencia *et al.*, "Virtual-Flux Finite Control Set Model Predictive Control of Switched Reluctance Motor Drives," in *IECON*, 2019, pp. 1301–1306.

[25] L. A. Serpa *et al.*, "A modified direct power control strategy allowing the connection of three-phase inverters to the grid through LCL filters," *IEEE Trans. Ind. Appl.*, vol. 43, no. 5, pp. 1388–1400, 2007.

[26] M. S. Grewal and K. Glover, "Identifiability of Linear and Nonlinear Dynamical Systems," *IEEE Trans. Autom. Control*, vol. 21, no. 6, pp. 833–837, 1976.

[27] A. Thowsen, "Identifiability of dynamic systems," *Int. J. Syst. Sci.*, vol. 9, no. 7, pp. 813–825, 1978.

[28] V. V. Nguyen and E. F. Wood, "Review and Unification of Linear Identifiability Concepts," *SIAM Rev.*, vol. 24, no. 1, pp. 34–51, 1982.

[29] S. Boyd and L. Vandenberghe, *Convex Optimization*, 7th ed. Cambridge University Press, 2009.

Michael Eull (S'12) received the B.Eng.Mgt. and MASc degrees from McMaster University, Hamilton, ON, Canada in electrical engineering. He is currently pursuing a PhD in electrical engineering at Columbia University in the City of New York, NY, USA, with a focus on state estimation for high performance control of power electronics and motor drives.

Matthias Preindl (S'12-M'15-SM'18) received the B.Sc. degree in electrical engineering (*summa cum laude*) from the University of Padua, Padua, Italy, the M.Sc. degree in electrical engineering and information technology from ETH Zurich, Zurich, Switzerland, and the Ph.D. degree in energy engineering from the University of Padua, in 2008, 2010, and 2014, respectively. He was an R&D Engineer of Power Electronics and Drives at Leitwind AG, Sterzing, Italy (2010-2012) and a Post Doctoral Research Associate and Sessional Professor in the Department of Electrical and Computer Engineering, McMaster University, Hamilton, ON, Canada (2014-2015). He is currently an Assistant Professor in the Department of Electrical Engineering, Columbia University, NY, USA.